

Remediation of Groundwater Contaminated with Copper Ions by Waste Foundry Sand Permeable Barrier

Ayad Abedalhamza Faisal

Assistant Professor

College of Engineering-University of Baghdad

Email: ayadabedalhamzafaisal@yahoo.com

Maryam Dheyauldeen Ahmed

MSc. student

College of Engineering-University of Baghdad

Email: maryam_dheya@yahoo.com

ABSTRACT

The permeable reactive barrier (PRB) is one of the promising innovative in situ groundwater remediation technologies, in removing of copper from a contaminated shallow aquifer. The 1:1-mixture of waste foundry sand (WFS) and Kerbala's sand (KS) was used for PRB. The WFS was represented the reactivity material while KS used to increase the permeability of PRB only. However, Fourier-transform infrared (FTIR) analysis proved that the carboxylic and alkyl halides groups are responsible for the sorption of copper onto WFS. Batch tests have been performed to characterize the equilibrium sorption properties of the (WFS+KS) mix in copper-containing aqueous solutions. The sorption data for Cu^{+2} ions, obtained by batch experiments, have been subjected to the Langmuir and Freundlich isotherm models. The Langmuir model was chosen to describe the sorption of solute on the solid phase of PRB. COMSOL Multiphysics 3.5a based on finite element method was used for formulation the transport of copper ions in two-dimension physical model under equilibrium condition. Numerical and experimental results proved that the PRB plays a potential role in the restriction of the contaminant plume migration. A good agreement between the predicted and experimental results was recognized with mean error (ME) not exceeded 10 %.

Keywords: groundwater, permeable reactive barrier, waste foundry sand, heavy metal, pollution.

معالجة المياه الجوفية الملوثة بأيونات النحاس بواسطة حاجز مخلفات رمل المسبك النفاذ

مريم ضياء الدين أحمد

طالبة ماجستير

كلية الهندسة - جامعة بغداد

أياد عبد الحمزة فيصل

أستاذ مساعد

كلية الهندسة - جامعة بغداد

الخلاصة

الحاجز التفاعلي النفاذ من التقنيات الحديثة المبتكرة لمعالجة المياه الجوفية في الموقع في إزالة عنصر النحاس من الطبقات السطحية الملوثة. خلطة مخلفات رمل المسبك ورمل كربلاء بنسبة (1:1) استخدمت كحاجز تفاعلي نفاذ حيث تمثل مخلفات رمل المسبك المادة الفعالة بينما يستخدم رمل كربلاء لزيادة نفاذية هذا الحاجز. التحليل باستخدام الأشعة تحت الحمراء أثبتت ان مجموعة الكربوكسيل وهاليدات الالكيل هي المسؤولة عن أمتزاز النحاس على مخلفات رمل المسبك. اختبارات الدفعة أنجزت لوصف صفات الأمتزاز للخلطة (مخلفات رمل المسبك ورمل كربلاء) في المحلول الحاوي على النحاس. البيانات التي تم الحصول عليها من التجارب بطريقة الدفعة تم تحليلها بواسطة موديلات لانكمير وفريندلج. تم اختيار موديل لانكمير لوصف أمتزاز المحلول على الطور الصلب للحاجز التفاعلي النفاذ. تم استخدام برنامج COMSOL Multiphysics 3.5 a الذي يعتمد على طريقة العناصر المحددة لوصف انتقال أيونات النحاس بموديل فيزيائي ثنائي الأبعاد في ظل حالة التوازن. النتائج المخبرية والعديدية أثبتت أن الحاجز التفاعلي النفاذ يلعب دور أساسي في حصر حركة البقعة الملوثة. لوحظ وجود توافق جيد بين النتائج المتوقعة والمخبرية وبمعدل خطأ أقل أو يساوي 10%.

الكلمات الرئيسية: المياه الجوفية، الحاجز التفاعلي النفاذ، مخلفات رمل المسبك، المعادن الثقيلة، التلوث.



1. INTRODUCTION

Groundwater is water found beneath the surface of the ground. It is primarily water that has seeped down from the surface by migrating through the soil matrix and spaces in geologic formations. Groundwater in aquifers is important for irrigation, domestic and industrial uses. Groundwater contamination can occur either from improper disposal, accidental releaseetc. or from naturally occurring mineral and metallic deposits in rock and soil. A groundwater pollutant is any substance that, when it reaches an aquifer, makes the water unclean or otherwise unsuitable for a particular purpose, **Mason, 2003**.

Heavy metals are among the most dangerous inorganic water pollutants, they can be related to many anthropogenic sources and their compounds are extremely toxic. These metals can be accumulated in the aquatic food web reaching human beings through the food chain, and causing several pathologies. The presence of heavy metals in groundwater is due to water exchange with contaminated rivers and lakes or to leaching from contaminated soils by rainfall infiltration, **Di Natale et al., 2008**.

The treatment of contaminated groundwater is among the most difficult and expensive environmental problems and often the primary factor limiting closure of contaminated sites. The most common technology used historically for remediation of groundwater has been ex-situ pump-and-treat systems. These systems are still suited for certain site-specific remediation scenarios; however, the limitations of pump-and-treat technologies have also been recognized. Accordingly, there was a necessity to develop other new innovative methods to remediate groundwater contaminated with heavy metals. Over the past decade, permeable reactive barriers (PRBs) have provided an increasingly important role in the passive interception and in-situ treatment of groundwater as a component of remedial action programs. PRBs have been used to remove a wide range of organic and inorganic contaminants from groundwater including petroleum hydrocarbons, chlorinated solvents, nutrients, metals and radionuclides, **Mountjoy et al., 2003**.

Bazdanis et al., 2011, studied the efficiency of PRBs containing organic material and limited quantities of ZVI, fly ash or red mud to remove heavy metals from leachates. Up-flow laboratory column experiments were carried out to study the efficiency in terms of Cu, Zn, Ni and Mn removal. The columns were filled with each reactive mixture and packed slightly to simulate field conditions; synthetic solutions with initial concentration of 50 mg/l of each metal were used. The experimental results showed in most cases adequate metal removal efficiency.

Chalermyanont et al., 2013, described performance of the PRBs on treating heavy-metal contaminated groundwater. ZVI and activated sludge were used as reactive media. Simulation results showed that funnel and gate PRBs have similar performance with the continuous PRBs on treating zinc contaminated groundwater but having less operation time. In additions, both ZVI and activated sludge can be used as reactive material with similar performance. The concentrations of zinc of treated groundwater are less than 5 mg/l.

However, the foundry industry releases large quantities of by-product WFS, which represent both a waste and a pollutant. For example, Nasr Company for Mechanical Industries, Special Steel Foundry / Iraq produced 10 tons of WFS per 8 hours when worked with full capacity. Thus, re-using of this waste as a reactive medium is attractive in terms of sustainable development, **Lee et al., 2004, Siddique et al., 2010 and Oliveira et al., 2011**. Thus, the significance of the present study are: (1) investigation the potential application of WFS as an inexpensive material in PRBs for the removal of copper (Cu^{2+}) from the contaminated groundwater; (2) determining the predominant functional groups which are responsible of Cu^{2+} removal in the WFS using Fourier transfer infrared spectroscopy (FTIR) analysis; and (3) characterization the 2D equilibrium transport of Cu^{2+} theoretically, using COMSOL

Multiphysics 3.5a (2008) software which is based on finite element method, and experimentally through simulated subsurface aquifer and WFS barrier under saturated condition for the equilibrium case.

2. MATERIALS AND METHODS

2.1 Materials

The WFS **Table 1** used in the present study had a particle size distribution ranged from 75 μm to 1 mm with an effective grain size, d_{10} , of 180 μm , a median grain size, d_{50} , of 320 μm and a uniformity coefficient, C_u , of 1.94. As the hydraulic conductivity of this sand was very low ($=1 \times 10^{-6}$ cm/s), it is mixed with Kerbala's sand (KS). The 1:1-mixture of (WFS+KS) was used with achieved conductivity equal to 2×10^{-3} cm/s. Also, the bulk density and porosity of this tested reactive mixture are 1.48 g/cm³ and 0.42 respectively.

The sandy soil, with composition and properties shown in **Table 2**, was used as aquifer in the conducted experiments. This soil had a particle size distribution ranged from 75 μm to 2 mm with an effective grain size, d_{10} , of 280 μm , a median grain size, d_{50} , of 240 μm and a uniformity coefficient, $C_u = d_{60}/d_{10}$, of 1.54.

Copper was selected as a representative of heavy metal contaminants. To simulate the water's copper contamination, a solution of $\text{CuSO}_4 \cdot 5\text{H}_2\text{O}$ (manufactured by Germany) was prepared and added to the specimen to obtain representative concentration.

2.2 Experimental Methodology

2.2.1 Batch experiments

Batch equilibrium tests are carried out to specify the best conditions of contact time, initial pH, initial concentration, (WFS+KS) dosage and agitation speed. Series of 250 ml flasks are employed and each flask is filled with 100 ml of copper solution which has initial concentration of 50 mg/l. One gram of (WFS+KS) was added into different flasks and these flasks were kept stirred in the high-speed orbital shaker at 250 rpm for 4 hours. A fixed volume (20 ml) of the solution was withdrawn from each flask. This withdrawn solution was filtered to separate the sorbent and a fixed volume (10 ml) of the clear solution was pipetted out for the concentration determination of the copper ion still present in solution. The measurements were carried out using atomic absorption spectrophotometer (AAS) (Norwalk, Connecticut (USA)) at the Center for Market Research and Consumer Protection. These measurements were repeated for two times and average value has been taken. However, the adsorbed concentration of metal ion on the (WFS+KS) was obtained by a mass balance.

The effect of various parameters such as initial pH (2, 4, 6.5, and 8), initial Cu^{2+} concentration (50, 100, 150, 200 and 250 mg/l), (WFS+KS) dosage (0.25, 0.5, 1, 3 and 5 g) and agitation speed (0, 50, 100, 150, 200 and 250 rpm) were studied in term of their effect on removal efficiency. The amount of metal ion retained on the (WFS+KS), q_e in (mg/g), was calculated as follows , **Wang et al. 2009**:

$$q_e = (C_o - C_e) \frac{V}{m} \quad (1)$$

where C_o is the initial concentration of copper in the solution (mg/l), C_e is the equilibrium concentration of copper remaining in the solution after the end of the experiment (mg/l), V is the volume of solution in the flask (l), and m is the mass of (WFS+KS) in the flask (g).

Langmuir Eq. (2) and Freundlich Eq. (3) models are used for the description of sorption data as follows , **Watts, 1998**:

$$q_e = \frac{abC_e}{1+bC_e} \quad (2)$$

where a is empirical constant and b is the saturation coefficient (l/mg).

$$q_e = K_F C_e^{1/n} \quad (3)$$

where K_F is the Freundlich sorption coefficient and n is an empirical coefficient.

2.2.2 Continuous experiments

The simulated Cu^{2+} transport was performed in a two-dimensional tank schematically shown in **Fig. 1**. This bench-scale model aquifer is contained within a rectangular 6 mm thick acrylic glass tank (100 cm L \times 40 cm W \times 10 cm D), including two vertical perforated acrylic glass plates as partitions covered with filter paper. These partitions are provided the lateral boundaries of the sand-filled middle compartment which has dimensions of 80 \times 40 \times 10 cm. The purpose of the two outer compartments, i.e. influent and effluent chambers, was controlling the position of the watertable within the model aquifer deposited in the middle compartment and, in addition, controlling the wetting of this aquifer mass. Each outer compartment has dimensions of 10 cm long, 40 cm width, and 10 cm high. The flow through the model aquifer was accomplished by peristaltic pump discharging copper solution from a storage tank of 10 l volume. One value of flow rate (120 ml/min) was selected here with corresponding interstitial velocity equal to (0.6 cm/min). Sampling plate **Fig. 2** was placed on the top of the glass tank to support the sampling ports. This plate contains 3 columns and 2 rows of sampling ports. Aqueous samples from the model aquifer were collected using stainless needles at specified periods.

The tank was packed with sandy soil as aquifer and (WFS+KS) as barrier in the configuration and alignment (10 cm thickness) illustrated in **Fig. 1**. Monitoring of Cu^{2+} concentration along the length of the tank in the effluent from sampling ports was conducted for a period of 3 days. Water samples of 2 ml volume were taken regularly (after 12, 24, 36... 72 hours) from these ports. For sampling the ports, six needles were connected to its location in each test. The samples were immediately introduced in test tubes and analyzed by AAS. The filling material in the middle compartment was assumed to be homogeneous and incompressible, and constant over time for water-filled porosity. All tubing and fitting for the influent and effluent lines should be composed of an inert material.

A tracer experiment in the tank described above was performed to determine the effective dispersion coefficient for the sandy soil and (WFS+KS) using the same procedure adopted by **Ujfaludi, 1986**.

A solution of 1 g/l NaCl in distilled water as a tracer was continuously fed into the tank. This tracer has been widely used due to its safety, cheapness, weak propensity to adsorption, not being affected by the liquids density and viscosity, and the easy detection of the concentration changes.

3. RESULTS AND DISCUSSION

3.1 Fourier-Transform Infrared (FTIR) Analysis

This analysis has been considered as a kind of direct means for investigating the sorption mechanisms by identifying the functional groups responsible for metal binding, **Chen et al., 2008**. Infrared spectra of WFS samples before and after sorption of Cu^{2+} were examined using (SHIMADZU FTIR, 800 series spectrophotometer). These spectra were measured within the range 4000-400 cm^{-1} as shown in **Fig. 3**. The sorption peaks in the region of 400-750 cm^{-1} can be assigned to $-\text{C}-\text{R}$ stretching vibrations of alkyl halides group. The carboxylic stretching

vibrations can be attributed to sorption peak at 1037.70. The shifts in the IR frequencies support that carboxylic and alkyl halides groups are responsible for the sorption of copper onto WFS, **Doke et al., 2012**.

3.2 Effect of Shaking Time and Initial pH of Solution

Fig. 4 shows the effect of contact time and initial pH of solution on Cu^{+2} sorption using 1 g of (WFS+KS) added to 100 ml of metal solution for batch tests at 25°C. This figure shows that the sorption rate was very fast initially and it's increased with increasing of contact time until reached the equilibrium time (= 1 h). This may be due to the presence of large number of adsorbent sites available for the sorption of metal ions. As the remaining vacant surfaces decreasing, the sorption rate slowed down due to formation of repulsive forces between the metals on the solid surfaces and in the liquid phase, **El-Sayed et al., 2010**. Also, the increase in the Cu^{+2} removal as the pH increases can be explained on the basis of a decrease in competition between proton and metal species for the surface sites which results in a lower columbic repulsion of the sorbing metal. However, further increase in pH values would cause a decreasing in removal efficiency. This may be attributed to the formation of negative copper hydroxides which are precipitated from the solution making true sorption studies impossible. It is clear from this figure that the maximum removal efficiency of copper was achieved at initial pH of 6.5.

3.3 Effect of (WFS+KS) Dose

Fig. 5 illustrates the Cu^{+2} removal efficiency as a function of different weights of (WFS+KS) ranged from 0.25 to 5 g added to 100 ml of metal solution. It can be observed that the removal efficiency improved with increasing (WFS+KS) dosage from 0.25 g to 1 g for a fixed initial metal concentration. This was expected due to the fact that the higher dose of adsorbents in the solution, the greater availability of sorption sites.

3.4 Effect of Agitation Speed

Fig. 6 shows that about 20% of the copper was removed before shaking (agitation speed= zero) and the uptake increases with the increase of shaking rate. There was gradual increase in metal ions uptake when agitation speed was increased from zero to 250 rpm at which about 93% of Cu^{+2} has been removed. This can be attributed to improving the diffusion of ions towards the surface of the reactive media and, consequently, proper contact between ions in solution and the binding sites can be achieved.

3.5 Sorption Isotherms

The sorption isotherms were produced by plotting the amount of copper removed from the solution (q_e in mg/g) against the equilibrium metal concentration in the solution (C_e in mg/l) at constant temperature, **Hamdaouia, and Naffrechoux, 2007** and **Kumar, and Kirthika, 2009**. The data of the batch tests are fitted with linearized form of Langmuir and Freundlich models. Accordingly, the equations of these models will be;

$$q_e = \frac{0.9292C_e}{1+0.092C_e} \quad R^2=0.988 \quad (4)$$

$$q_e = 3.397C_e^{0.207} \quad R^2=0.986 \quad (5)$$

It is clear that these models are provided the best representation of copper sorption onto (WFS+KS) reactive material. However, the Langmuir model was chosen to describe the

sorption of solute on solid in the partial differential equation governed the transport of a solute undergoing equilibrium sorption through permeable reactive barrier in the continuous mode.

3.6 Longitudinal Dispersion Coefficient

Results of the experimental runs concerned the measurement of longitudinal dispersion coefficient (D_L) at different values of velocity (V) for soil and (WFS+KS) are taken a linear relationship as follows:

For soil,

$$D_L = 68.16 V + 0.056 \quad R^2=0.973 \quad (6)$$

For (WFS+KS),

$$D_L = 73.51 V + 0.282 \quad R^2=0.999 \quad (7)$$

These equations are taken the general form of longitudinal hydrodynamic dispersion coefficient as follows:

$$D_L = \alpha_L V + \tau D_o \quad (8)$$

This means that the longitudinal dispersivity (α_L) is equal to 68.16 cm for soil and 73.51 cm for mix.

3.7 2D PRB design-model setup

The contaminant migration in a porous medium is due to advection-dispersion processes; therefore, considering a two dimensional system, the dissolved copper mass balance equation may be written, as follows:

$$D_x \frac{\partial^2 C_{cu}}{\partial x^2} + D_y \frac{\partial^2 C_{cu}}{\partial y^2} - V_x \frac{\partial C_{cu}}{\partial x} = R \frac{\partial C_{cu}}{\partial t} \quad (9)$$

where C_{cu} represents copper mass concentration in water and R is known as the retardation factor since it has the effect of retarding the transport of adsorbed species relative to the advection front..

For the flow of contaminated groundwater through the sandy soil, the value of R will be assumed equal to 1 which is reasonable for this type of soils. On the other hand, the sorption of copper on (WFS+KS) barrier is governed by Langmuir sorption isotherm and the retardation factor is expressed as:

$$R = 1 + \frac{\rho_d}{n_B} \left(\frac{0.9292}{(1+0.092C_{cu})^2} \right) \quad (10)$$

where n_B is the porosity of the barrier.

To present theoretical verification for tank test described previously, Eq. (9) in combination with initial and boundary conditions **Table 3** can be solved using COMSOL Multiphysics 3.5a. The used mesh discretization (i.e. number of mesh points, number of elements, and type of elementsetc) is shown in **Fig. 7**.

Fig. 8 plotted the predicted spatial distribution of copper normalized concentration across the sand aquifer in the presence of (WFS+KS) barrier after 7 days for flow rate equal to 60 and 120

ml/min. It is clear that the propagation of contaminated plume is restricted by this barrier region. Also, the value of applied flow rate, i.e. velocity of flow, plays a significant role in the extent and concentration magnitude of the contaminant plume. Accordingly, the extent of contaminant plume in the longitudinal (x) direction is greater than transverse (y) direction and highest concentrations occur in the sand bed which up-gradient of PRB. The concentration of the contaminated plume reaching the outlet may attain lower than 1.3 mg/l quality limit prescribed for surface water or drinking water, **Hashim et al., 2011**.

Comparisons between the predicted and experimental results at nodes corresponding to monitoring ports during the migration of the Cu^{+2} plume at different periods of time for flow rate equal to 120 ml/min using (WFS+KS) barrier are depicted in **Fig. 9**. Although the spatial and temporal concentration profiles are taken the same trend, concentration values in the ports (1, 2, and 3) located along the centerline of the source area ($y=20$ cm) are greater than that in the ports (4, 5, and 6) deviated from the centerline by 10 cm (i.e. $y=10$ cm). Also, it is clear that the (WFS+KS) barrier have a potential functionality in the retardation of the contaminant migration in the down gradient of this barrier (concentration at ports 3 & 6 equal approximately zero). However, a reasonable agreement between the predicted and experimental results can be observed with ME less than 10%.

4. CONCLUSIONS

- ❖ Contact time, initial pH of the solution, initial metal ion concentration, (WFS+KS) dose and agitation speed were most the parameters affected on the sorption process between Cu^{+2} ions and (WFS+KS). The best values of these parameters that will achieve the maximum removal efficiency of Cu^{+2} (=93%) were 1 h, 6.5, 50 mg/l, 1 g/100 ml, and 250 rpm respectively.
- ❖ The experimental data for copper sorption on the (WFS+KS) were correlated well by the Langmuir isotherm model with coefficient of determination (R^2) equal to 0.986.
- ❖ FTIR analysis proved that the carboxylic and alkyl halides groups are responsible for the sorption of copper onto WFS.
- ❖ The results of 2D numerical model solved by COMSOL Multiphysics 3.5a under equilibrium condition proved that the (WFS+KS) barrier is efficient technique in the restriction of contaminant plume. However, a good agreement between the predicted and experimental results was recognized with ME not exceeded 10 %.

REFERENCES

- Bazdanis, G., Komnitsas, K., Sahinkaya, E., and Zaharaki, D., 2011, *Removal of Heavy Metals from Leachates Using Permeable Reactive Barriers Filled with Reactive Organic/Inorganic Mixtures*, Proceedings of the 3rd International Conference on Environmental Management, Engineering, Planning, and Economics (CEMEPE 2011) & SECOTOX Conference, Skiathos island, Greece (19-24 June).
- Chalermyanont, T., Chetpattananondh, P., and Riyapan, N., 2013, *Numerical Modeling of Permeable Reactive Barriers to Treat Heavy-Metal Contaminated Groundwater*, 6th PSU-UNS International Conference on Eng. and Tech. (ICET_2013), Novi Sad, Serbia, University of Novi Sad, Faculty of Technical Sciences.



- Chen, J. P., Wang, L., and Zou, S. W., 2008, *Determination of Lead Bio-sorption Properties by Experimental and Modeling Simulation Study*, Chemical Eng. J., 131, 209-215.
- Di Natale, F., Di Natale, M., Greco, R., Lancia, A., Laudante, C., and Musmarra, D., 2008, *Groundwater Protection From Cadmium Contamination by Permeable Reactive Barriers*, J. Hazard. Mater., 160, 428–434.
- Doke, K. M., Yusufi, M., Joseph, R. D., and Khan, E. M., 2012, *Bio-sorption of Hexavalent Chromium onto Wood Apple Shell: Equilibrium, Kinetic and Thermodynamic Studies*, Desalination and Water Treatment, 50, 170-197.
- El-Sayed, G. O., Dessouki, H. A., and Ibrahim, S. S., 2010, *Bio-sorption of Ni(II) and Cd(II) Ions from Aqueous Solutions onto Rice Straw*, Chem. Sci. J., CSJ-9.
- Hamdaoui, O., and Naffrechoux, E., 2007, *Modeling of Adsorption Isotherms of Phenol and Chlorophenols onto Granular Activated Carbon*, J. Hazard. Mater., 147, 381–394.
- Hashim, M. A., Mukhopadhyay, S., Sahu, J. N., and Sengupta, B., 2011, *Remediation Technologies for Heavy Metal Contaminated Groundwater*, J. of Environmental Management, 92, 2355-2388.
- Kumar, P. S., and Kirthika, K., 2009, *Equilibrium and Kinetic Study of Adsorption of Nickel from Aqueous Solution onto Bael Tree Leaf Powder*, J. Eng. Sci. and Tech., 4, 351-363.
- Lee, T., Benson, C. H., and Eykholt, G. R., 2004, *Waste Green Sands as Reactive Media for Groundwater Contaminated with Trichloroethylene (TCE)*, J. Hazard. Mater., B109, 25-36.
- Mason, W.R., 2003, *Pollution of Groundwater*, www.encyclopedia.com › ... › Water: Science and Issues › January 2003.
- Mountjoy, K.J., Pringle, E.K., Choi, M., and Gowdy, W., 2003, *The Use of Permeable Reactive Barriers for In-situ Remediation of Groundwater Contaminants*, www.esaa-events.com/remtech/2003/pdf/Mountjoy.pdf.
- Oliveira, P. E. F., Oliveira, L. D., Ardisson, J. D., and Lago, R. M., 2011, *Potential of Modified Iron Rich Foundry Waste for Environmental Applications: Fenton Reaction and Cr(VI) Reduction*, J. Hazard. Mater., 194, 393-398.
- Siddique, R., Kaur, G., and Rajor, A., 2010, *Waste Foundry Sand and its Leachate Characteristics*, Resources, Conservation and Recycling, 54, 1027-1036.
- Ujfaludi, L., 1986, *Longitudinal Dispersion Tests in Non-uniform Porous Media*, Hydrological Sciences - Journal - des Sciences Hydrologiques, 31.



- Wang, S., Nan, Z., Li, Y., and Zhao, Z., 2009, *The Chemical Bonding of Copper Ions on Kaolin from Suzhou, China*, *Desalination* ,249 ,991–995.
- Watts, R.J., 1998, *Hazardous Wastes: Sources, Pathways, Receptors*, John Wiley and Sons, Inc.

NOMENCLATURE

a: empirical constant , l/g.
b: saturation coefficient , mg/g.
 C_{cu} : copper concentration , mg/l.
 C_o : initial concentration , mg/l.
 C_e : equilibrium concentration , mg/l.
 C_u : uniformity coefficient , dimensionless.
 D_L : longitudinal hydrodynamic dispersion coefficient , m^2/sec .
 D_o : molecular diffusion coefficient , m^2/sec .
 D_x : longitudinal dispersion coefficient , m^2/sec .
 D_y : lateral dispersion coefficient , m^2/sec .
 K_F : freundlich sorption coefficient , m^2/sec .
 m :mass of (WFS+KS) in the flask , g.
 n : porosity ,dimensionless.
 q_e : amount of solute removed from solution , mg/kg.
R: retardation factor,dimensionless.
 R^2 : coefficient of determination
V : volume of solution in the flask , l.
 V_x : actual velocity , m/sec.
 τ : tortuosity factor of soil medium
 ρ_b : bulk density of the soil , g/cm^3 .
 α_L : longitudinal dispersivity , cm.

**Table 1.** Composition and physico-chemical properties of WFS.

Property	Value
SiO ₂ (%)	94.36
Al ₂ O ₃ (%)	2.82
Fe ₂ O ₃ (%)	2.12
Na ₂ O (%)	0.24
CaO (%)	0.05
TiO ₂ (%)	0.14
MgO (%)	0.23
K ₂ O (%)	0.039
Bulk density (g/cm ³)	1.44
Particle density (g/cm ³)	2.67
Porosity	0.46
Surface area (m ² /g)	5.9351
Cation exchange capacity (meq/100 g)	10.94

Table 2. Composition and properties of the soil used in the present study.

Property	Value
Particle size distribution (ASTM D 422) Sand (%) Silt and Clay (%)	99 1
Hydraulic conductivity (cm s ⁻¹)	2x10 ⁻³
Cation exchange capacity (meq/100 g)	3.12
pH	8.5
Organic content (ASTM D 2974, %)	0.26
Bulk density (g/cm ³)	1.567
Porosity	0.409
Soil classification	Sand

Table 3. Boundary and initial conditions used in the transport modeling of copper in 2D laboratory scale tank.

Item	Location	Type/ Value
Boundary conditions	Upper boundary	No flux/symmetry
	Lower boundary	No flux/symmetry
	Left side boundary	No flux/symmetry
	Right side boundary	Advective flux
	Line source	Concentration=50 mg/l
Initial condition	(x,y)	Concentration=0

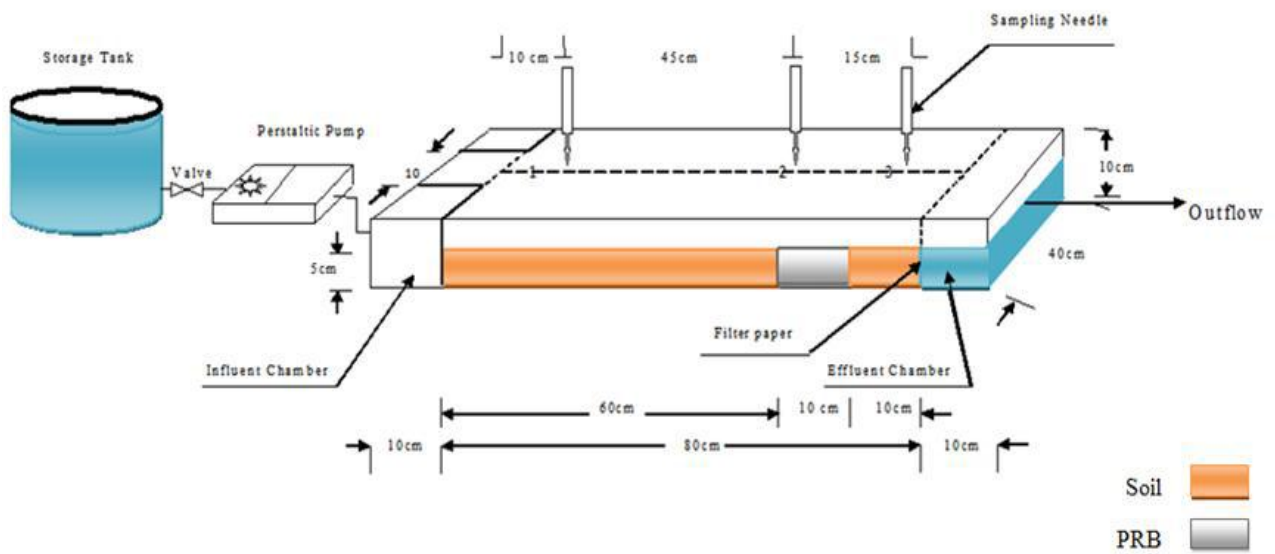


Figure 1. Schematic diagram of the bench-scale model aquifer.

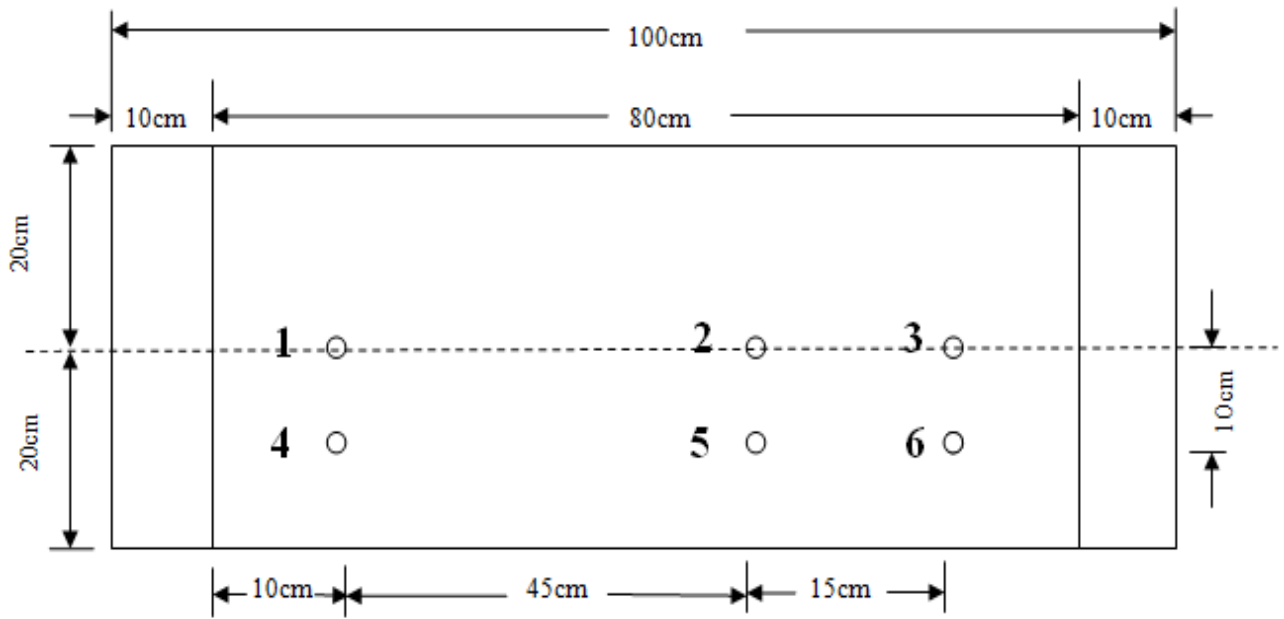


Figure 2. Schematic diagram of the sampling plate and sampling ports.

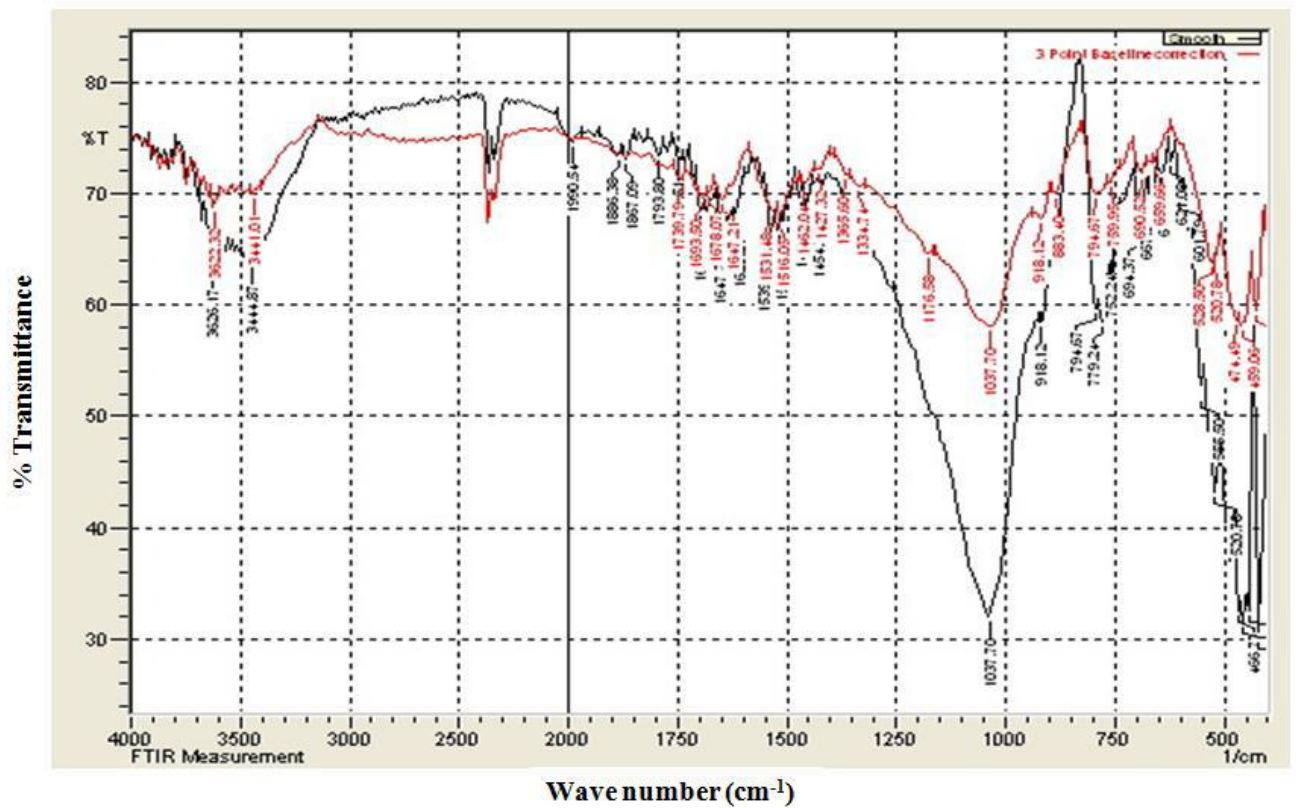


Figure 3. FTIR spectra of WFS (black line) before sorption and (red line) after sorption.

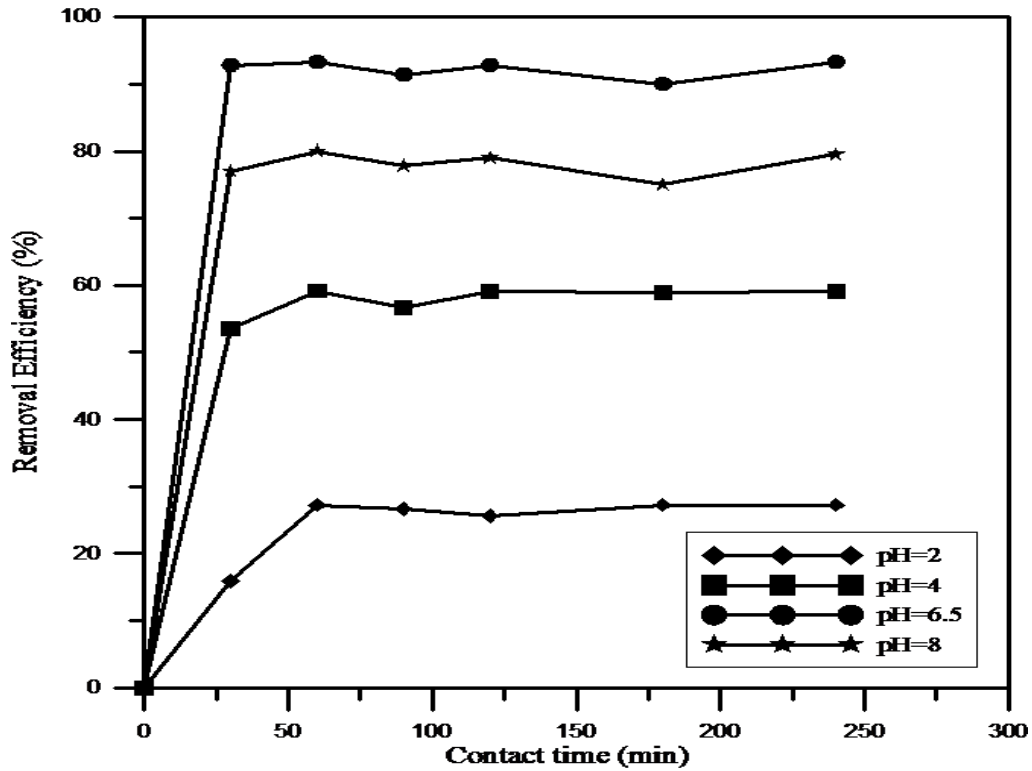


Figure 4. Effect of initial pH on removal efficiency of copper by (WFS+KS) as a function of contact time ($C_0=50$ mg/l; (WFS+KS) dose= 1 g/100 ml; agitation speed= 250 rpm; $T=25^\circ\text{C}$).

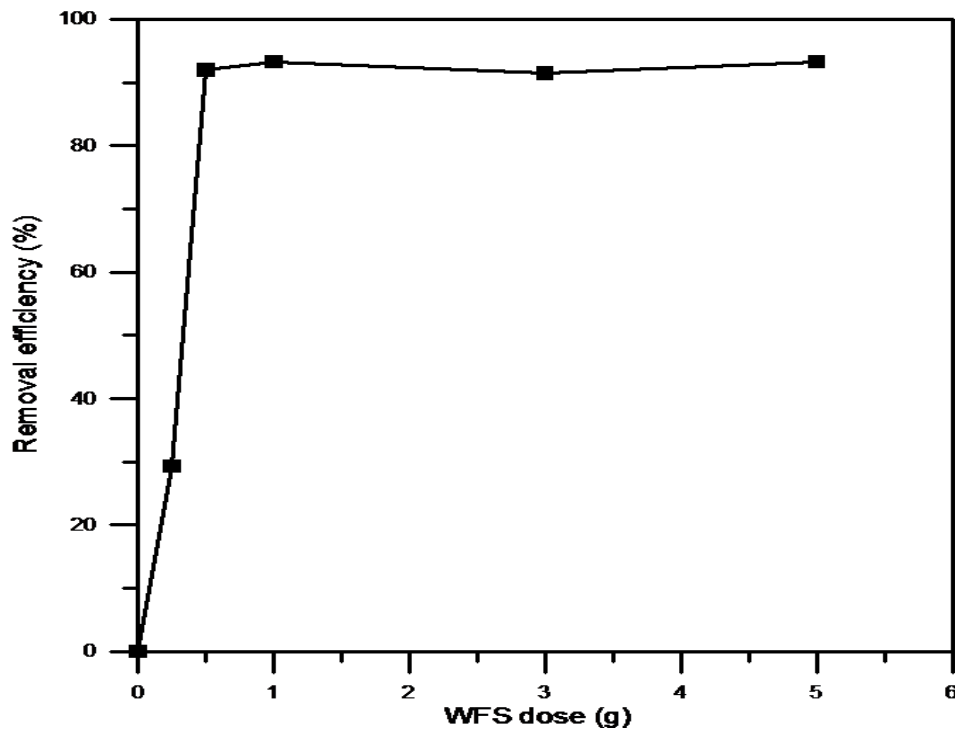


Figure 5. Effect of WFS dosage on removal efficiency of copper ($C_0=50$ mg/l; pH=6.5; agitation speed= 250 rpm; contact time=1 h; $T=25^\circ\text{C}$).

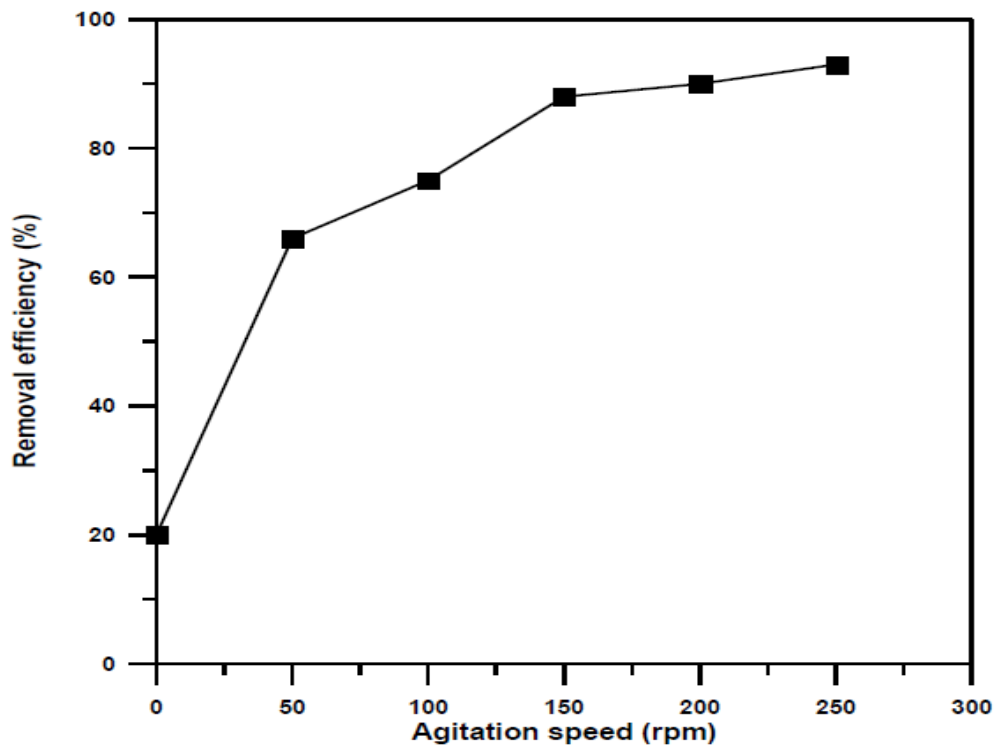


Figure 6. Effect of agitation speed on removal efficiency of copper as a function of contact time ($C_o=50$ mg/l; pH=6.5; WFS dose= 1 g/100 ml; T= 25°C).

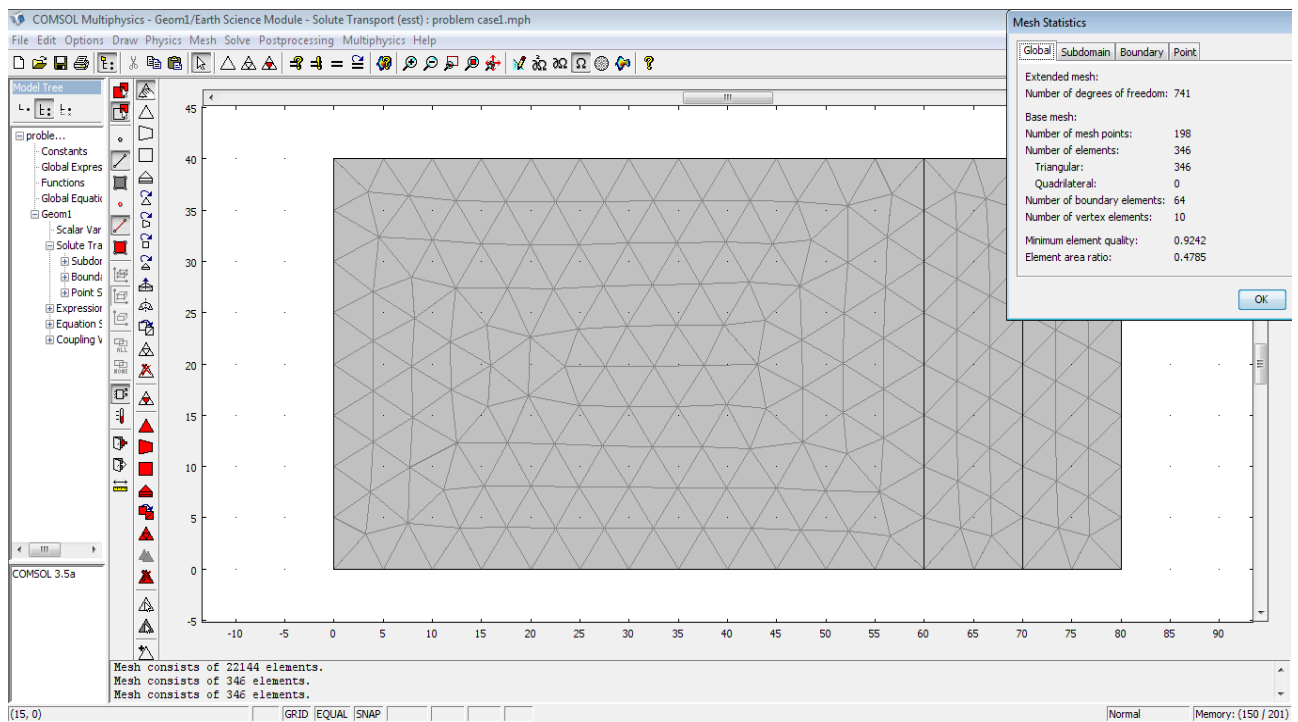


Figure 7. Domain discretization and mesh statistics of 2D model (all dimensions in cm).

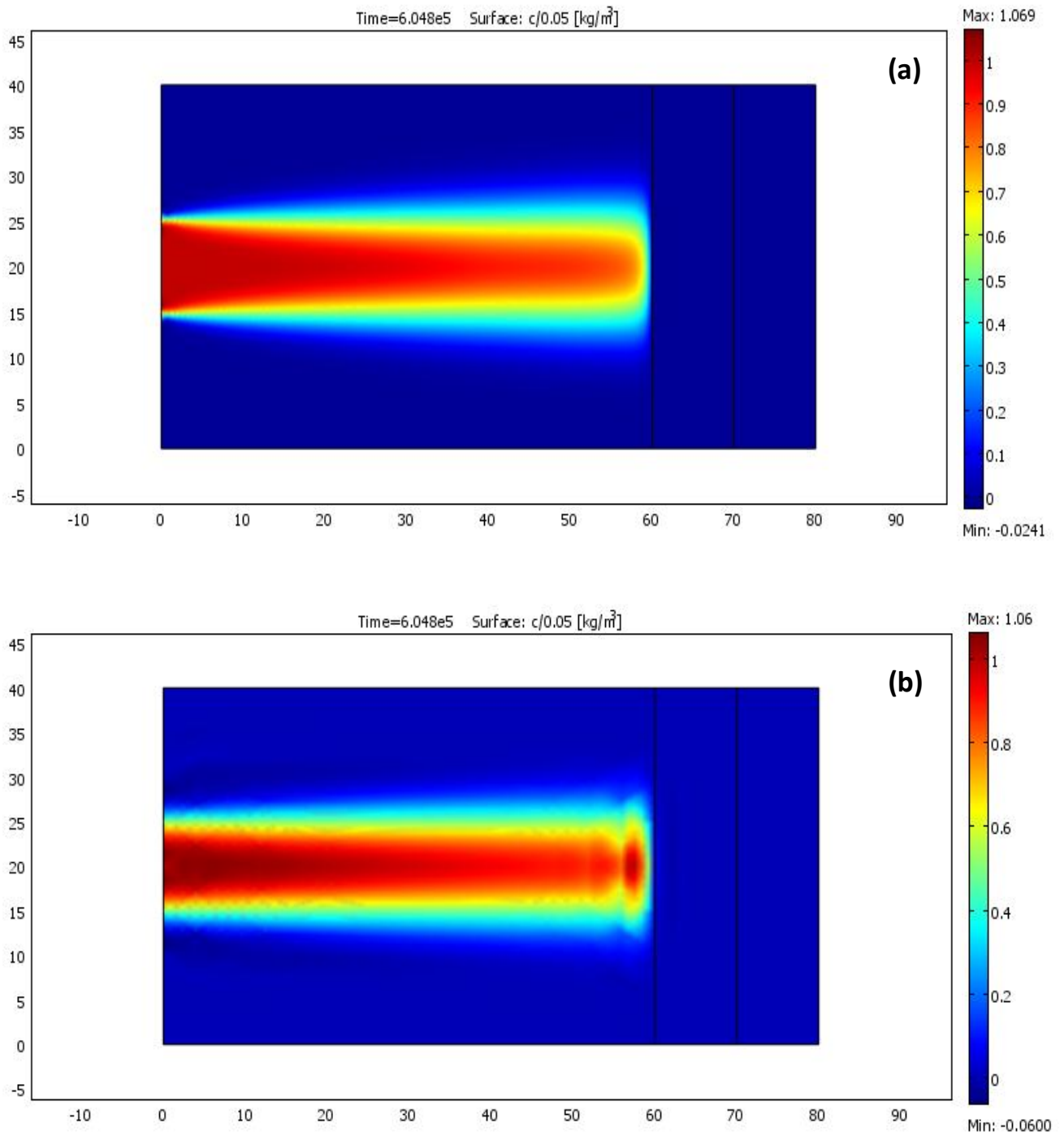


Figure 8. Distribution of copper concentration after 7 days for flow rate equal to (a) 60 and (b) 120 ml/min.

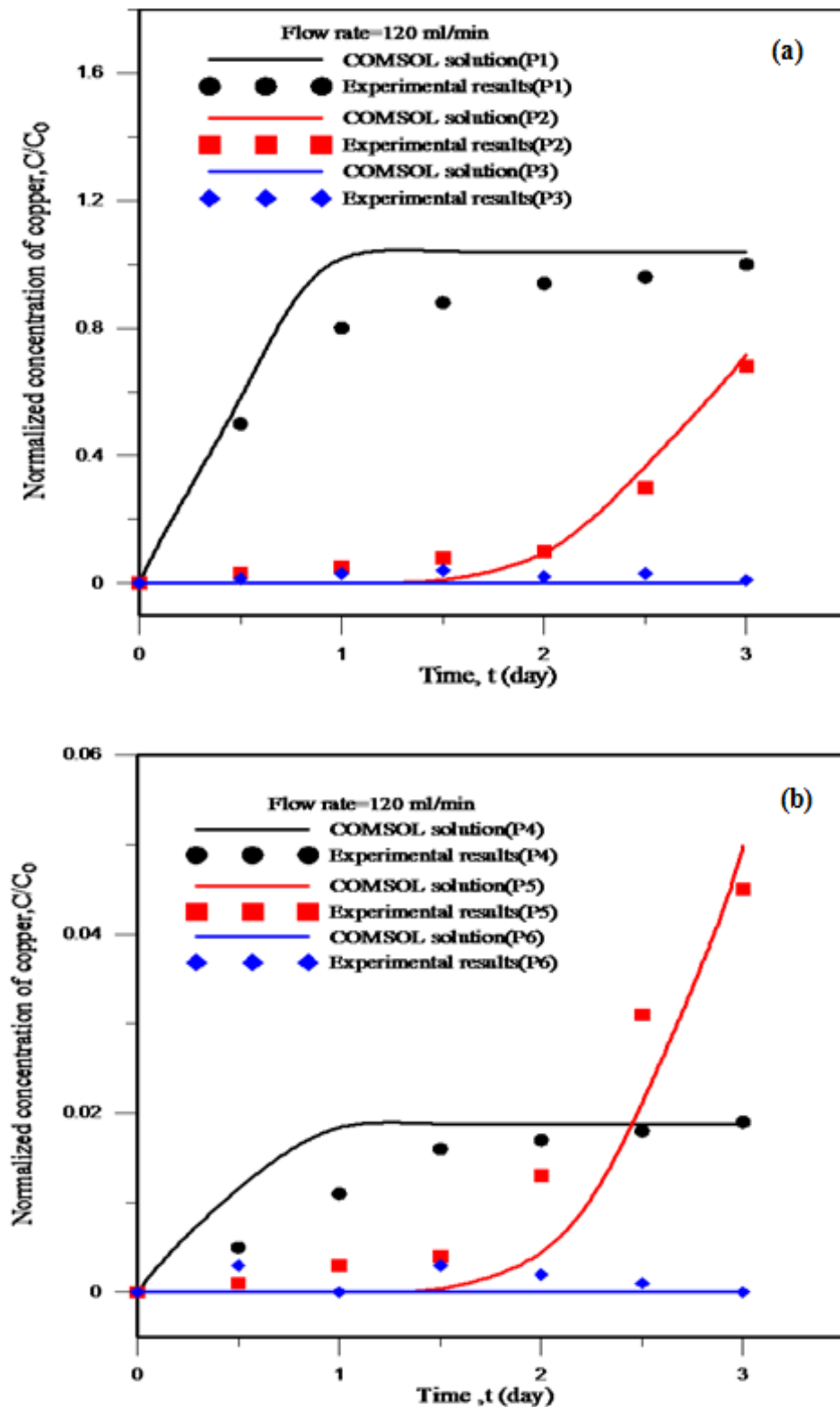


Figure 9. Breakthrough curves as a result of the copper transport at different ports located at (a) $y=20$ and (b) $y=10$ cm for flow rate=120 ml/min.